

Implications of Energy Profile and Storage on Energy Harvesting Sensor Link Performance

Bhargav Medepally Neelesh B. Mehta, *Senior Member, IEEE* Chandra R. Murthy, *Member, IEEE*

Abstract—Energy harvesting sensors (EHS), which harvest energy from the environment in order to sense and then communicate their measurements over a wireless link, provide the tantalizing possibility of perpetual lifetime operation of a sensor network. The wireless communication link design problem needs to be revisited for these sensors as the energy harvested can be random and small and not available when required. In this paper, we develop a simple model that captures the interactions between important parameters that govern the communication link performance of a EHS node, and analyze its outage probability for both slow fading and fast fading wireless channels. Our analysis brings out the critical importance of the energy profile and the energy storage capability on the EHS link performance. Our results show that properly tuning the transmission parameters of the EHS node and having even a small amount of energy storage capability improves the EHS link performance considerably.

I. INTRODUCTION

Wireless energy harvesting sensor networks, in which the sensor nodes harvest energy from the environment, offer the promise of perpetual operation without requiring external power cables or periodic battery replacements. Each node can use solar, vibration, thermoelectric effects, and other phenomena to harvest the energy it requires to carry out its sensing, signal processing, communication, and network maintenance related tasks [1]. Consequently, these networks have applications in environmental and industrial monitoring, intrusion detection, etc. However, energy harvesting poses new problems related to link and network design. This is because the harvested energy might be available in random amounts and only sporadically. Therefore, problems specific to EHS links are now being addressed in the literature [2]–[5].

A key aspect that affects EHS link performance is the *energy profile*, which models the availability of energy with time at an EHS node. The energy profile and its parameters, in general, depend on the device physics [6]. Various analytical models for it have been considered. For example, a leaky bucket model motivated by Internet traffic modeling was used in [6], in which the rate of harvesting is known accurately but at any time there is an uncertainty in the total energy that can be harvested. A Bernoulli model was used in [5], in which energy is harvested with a fixed probability. A Markov model has also been used [2].

Another important component that affects the EHS link performance is the ability of the EHS node to temporarily

store excess harvested energy in a battery and utilize this energy later. Doing so enables the node to overcome the randomness in energy availability, and, thus, improves the link performance. Consequently, the EHS link performance depends on both the energy profile and the energy storage of the EHS node.

In this paper, we analytically characterize the communication performance of an EHS link as a function of the EHS node's energy profile parameters and its battery's energy storage capability, if any. Specifically, we consider an EHS node that needs to periodically transmit measurement information to a destination node over a time-varying wireless fading channel. We derive expressions for the outage probability for both slow fading and fast fading channels. Our analysis and modeling clearly brings out the important interactions that occur between various system parameters in an EHS link. Based on the analysis, we also optimize the transmission parameters of the node to minimize the outage probability. Our results show that it is important to correctly tune communication parameters such as the transmit energy per measurement to the energy profile and battery capacity of the EHS node.

The paper is organized as follows. Section II sets up the system model. The EHS link performance with and without energy storage is characterized in Sections III and IV, respectively. Simulation results are presented in Section V, and are followed by our conclusions in Section VI.

II. MODEL

We consider an EHS node that needs to transmit a measurement of D data bits periodically every T_m sec to a destination node over a time-varying wireless fading channel. The EHS node encapsulates its data bits in a packet of duration T_p sec. The packet also contains a synchronization header of S bits (and of duration T_{sync}) to enable the receiver to synchronize easily. In order to enable easy synchronization and reception, we take the bits to be on-off keying (OOK) encoded, as done in [7]. Each OOK symbol is of duration T_s . Note that the analysis easily extends to other linear modulations.

The EHS node continues to retransmit the packet until it receives an acknowledgment (ACK) from the receiver or it is time to transmit the next measurement. A measurement *outage* occurs if the node fails to deliver the packet to the destination successfully within time T_m . The waiting time, T_w , at the transmitter for receiving an ACK is taken to be negligible; but, the analysis can easily be extended to handle this by including

The authors are with the Electrical Communication Engineering Dept. at the Indian Institute of Science (IISc), Bangalore, India.
Emails: {bhargav, nbmehta, cmurthy}@ece.iisc.ernet.in

the waiting time in T_p . Thus, within the m th measurement interval $[mT_m, (m+1)T_m)$, transmissions/retransmissions occur at times $mT_m, mT_m + T_p, \dots, mT_m + (K-1)T_p$, where $K = \lfloor \frac{T_m}{T_p} \rfloor$ is the total number of transmissions (including retransmission) possible.

No channel state information is assumed to be available at the transmitting EHS node as acquiring this information is energy expensive and complicates the system design. Therefore, the node transmits its packets with a fixed power P , which is a static system parameter.

In order to enable analytical tractability and gain insights, we now make some simplifying assumptions in our model. These simplifications bring out the key interactions and trade-offs that need to be considered when optimizing EHS link performance. The packets are taken to be uncoded. The case of coded packet transmission is beyond the scope of this paper and is considered in [8]. We focus on the transmit energy consumption in this paper since it is the dominant component when the inter-sensor distances are relatively large [9].

We hereafter use the term ‘slots’ to refer to intervals of duration T_p , and discretize time in multiples of T_p .

A. Energy Harvesting Model (Energy Profile)

We assume a probabilistic model similar to [5] in which an energy E_s is harvested and available at the beginning of every slot with probability ρ . With probability $1 - \rho$ no energy is harvested. Both E_s and ρ depend on the harvesting mechanism. We assume that the energy harvested in each slot is identical and independently distributed. A more refined model would allow for multiple levels of harvested energy and also model time correlations, if any. While the above model is simple, it does capture the sporadic and random availability of energy at an EHS node. The model is motivated by switch-based or vibration-based harvesting mechanisms [10].

B. Channel Model

We assume a block fading Rayleigh channel. The efficacy of retransmissions depends on the coherence time, T_c , of the channel. We, therefore, consider the following two cases:

- *Slow fading*: The channel gain remains the same during the entire measurement interval, T_m . Consequently, all retransmissions of a packet see the same channel. This occurs when $T_c \approx T_m$. This corresponds to a low mobility environment.
- *Fast fading*: The channel gain changes from one packet transmission to another (but remains the same within a packet). This occurs when $T_c \approx T_p$, and corresponds to a highly mobile environment in which the packet transmissions are frequent enough to span the coherence time.

The instantaneous SNR, γ , at the destination receiver is

$$\gamma = \left(\frac{d_0}{d}\right)^\eta |h|^2 \frac{PT_s}{N_0}, \quad (1)$$

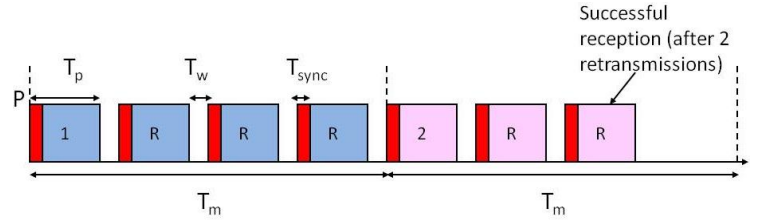


Fig. 1. Periodic packet transmission model of the EHS node.

where d_0 is a reference distance, η is the propagation exponent, and N_0 is the noise spectral density. The Rayleigh channel power gain, $|h|^2$, is an exponentially distributed random variable with unit mean. Therefore, the average SNR equals $\bar{\gamma} = \left(\frac{d_0}{d}\right)^\eta PT_s/N_0$. (Slowly varying shadowing, if present, can be factored into the d_0 term; it is, therefore, not shown here explicitly.)

C. Energy Storage

We consider two scenarios. In the first is an extreme scenario that serves primarily as a benchmark. In it, the energy harvested over a short duration cannot be stored by the EHS node and must be used up immediately or discarded. In the second case, a battery is available to accumulate excess energy for subsequent transmissions.

We now evaluate the outage probability of an EHS link as a function of the energy storage capability of the EHS node.

III. WITHOUT STORAGE BUFFER

When a storage buffer is absent, the best strategy for the node is to transmit, if possible, using all the harvested energy available for that slot. Hence, the transmit power, P , equals $PT_p = E_s$. Outage occurs if the destination does not receive a packet by the end of the measurement interval (K slots).¹

The channel-averaged probability of outage for a payload of D data bits per packet is given in closed-form below.

Proposition 1: The probability of outage of a EHS link in a slow fading Rayleigh channel is given by (3), where A_r is the coefficient of y^r in the series expansion of $(1 + \rho(1 - y)^D)^K$, $\Gamma(\cdot)$ is the gamma function, and $F_A^n(\dots)$ is the Lauricella hyper-geometric function of n variables [11].

Proof: An outage occurs when either there is insufficient energy to transmit a packet or the packet is received in error. Therefore, the channel-averaged outage probability equals

$$P_{\text{out}} = \mathbf{E}_\gamma \left[\left(1 - \rho + \rho \left(1 - (1 - Q(\sqrt{\gamma}))^D \right) \right)^K \right]. \quad (2)$$

This follows because the symbol error probability for OOK is $Q(\sqrt{\gamma})$. The desired result is obtained by expanding the integrand above, and using the Lauricella hyper-geometric closed-form result from [13] to evaluate $\int_0^\infty Q^r(\sqrt{\gamma}) f_\gamma(\gamma) d\gamma$. ■

A similar expression can be derived for fast fading. It involves first averaging $P_e(\gamma)$ over the distribution of γ .

¹The probability of outage due to synchronization header corruption is significantly lower, and is, therefore, not considered.

$$P_{\text{out}} = \sum_{r=0}^{DK} \frac{A_r}{2^r} - \sum_{r=0}^{DK} \frac{rA_r}{2^r} \sqrt{\frac{\bar{\gamma}}{\bar{\gamma}+2}} - \sum_{r=0}^{DK} \frac{A_r}{2^r} \frac{r}{\sqrt{2\pi}} \sum_{n=1}^{r-1} \Gamma\left(\frac{n+1}{2}\right) \binom{r-1}{n} (-1)^n \left(\frac{\bar{\gamma}}{\sqrt{2\pi}}\right)^n \times \left(\frac{2\bar{\gamma}}{(n+1)\bar{\gamma}+2}\right)^{\frac{n+1}{2}} F_A^{(n)}\left(\frac{n+1}{2}, \underbrace{1, \dots, 1}_{n \text{ terms}}; \underbrace{\frac{3}{2}, \dots, \frac{3}{2}}_{n \text{ terms}}; \underbrace{\frac{\bar{\gamma}}{(n+1)\bar{\gamma}+2}, \dots, \frac{\bar{\gamma}}{(n+1)\bar{\gamma}+2}}_{n \text{ terms}}\right). \quad (3)$$

IV. WITH STORAGE BUFFER

In the n th slot, the node transmits a packet with power P if the available energy, B_n , in the battery exceeds PT_p , the energy required to transmit a packet at power P . Otherwise, no packet transmission occurs. *Note that after receiving a successful ACK, the node no longer needs to retransmit the packet. Instead, it just accumulates the energy harvested during the rest of the measurement interval and waits for the start of the next interval.* In general, depending on the system parameter settings, $W = E_s/PT_p$ can be any real number. The cases where $W = 1/L < 1$ and $W = L \geq 1$, where L is an integer, are analyzed below. The analysis can be generalized to handle the case where W is a rational number. W is a system parameter that needs to be optimized. The treatment is brief due to tight space constraints. Details and derivations are given in [8].

A. Case 1: Fractional Energy Harvested ($E_s = PT_p/L$)

When the EHS node transmits in a slot, its energy decreases by LE_s . The outage analysis for the slow fading and fast fading cases turn out to be slightly different. We treat them separately below.

1) *Slow Fading*: Recall that in slow fading, the channel state remains the same within a measurement interval and changes to an independent value thereafter. Given the energy profile model assumed, a key observation that enables analysis is that the process *within a measurement interval and given the SNR, γ* , is a discrete time Markov process. This is shown in Fig. 2. The state is defined by two variables: (i) the energy (normalized with respect to E_s) stored in the battery, B_n , and (ii) the feedback state, U_n , where $U_n = 0$ if no ACK arrived within the measurement interval, and is 1 otherwise.

At the beginning of the m th measurement interval (*i.e.*, time slot mK), the node is always in a state $(B_{mK}, 0)$ since an ACK is yet to arrive. It transitions to a $(B_n, 1)$ state once an ACK arrives in slot n of the measurement interval. Also, it no longer transmits in the remaining slots of the measurement interval. The total number of states equals $2(\lceil C/E_s \rceil + 1)$, where C is the battery's storage capacity. Irrespective of the feedback state at the end of the m th interval, the energy state at the beginning of the $(m+1)$ th interval is the same as that at end of the m th interval, and the feedback state at the beginning of the $(m+1)$ th interval is always 0. For this reason, the Markov chain above is valid only within a measurement interval.

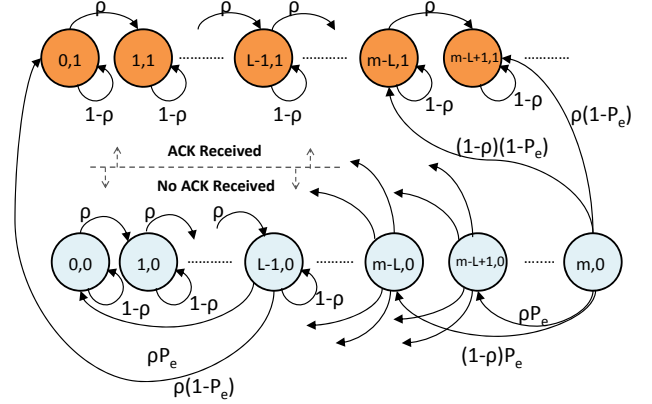


Fig. 2. Discrete time Markov evolution of battery and transmission states within a measurement interval (when $E_s = PT_p/L$).

Outage occurs in a measurement interval if and only if the node is in a $U_n = 0$ state at the end of the interval. Since B_{mK} is independent of the channel in $[mK, (m+1)K)$, the outage probability, as a function of $K \geq 1$, is given by

$$P_{\text{out}}(K) = \sum_i \pi(i) \mathbf{E}_\gamma [P_{\text{out}}(K|i, \gamma)], \quad (4)$$

where $\pi(i)$ is the stationary probability that the node has energy iE_s at the beginning of a measurement interval and $\mathbf{E}_\gamma[\cdot]$ is the expectation operator. (The non-stationary case, which turns out to be easier, is handled in Appendix C.) From the Markov structure, the outage probability as a function of K ($K \geq 1$) and conditioned on the SNR, γ , and $B_{mK} = iE_s$ obeys the following recursion relation:

$$P_{\text{out}}(K|i, \gamma) = \begin{cases} \sum_{r=0}^K \binom{K}{r} \rho^r (1-\rho)^{K-r} P_e^{\lfloor \frac{i+r}{L} \rfloor}(\gamma), & i \leq L-1 \\ \rho P_e(\gamma) P_{\text{out}}(K-1|i-L+1, \gamma) + (1-\rho) P_e(\gamma) P_{\text{out}}(K-1|i-L, \gamma), & i \geq L \end{cases}$$

This is because for $i < L$, r energy injections lead to $\lfloor \frac{i+r}{L} \rfloor$ packets getting transmitted. For $i \geq L$, a packet transmission will occur and use up energy LE_s . Thereafter, the next state's energy is either $(m-L)$ or $(m-L+1)$ depending on whether an energy injection occurs or not in the same slot. We also have $P_{\text{out}}(0|i, \gamma) = 1$.

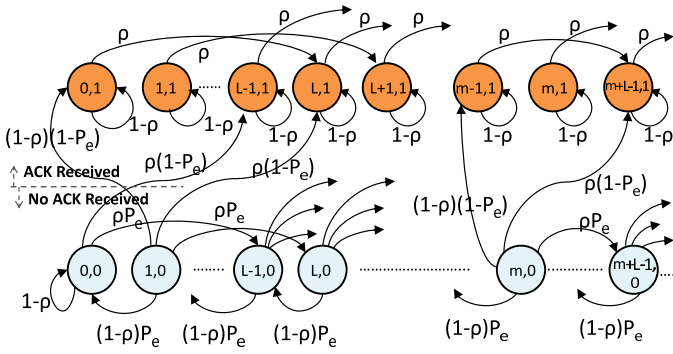


Fig. 3. Discrete time Markov evolution of battery and transmission states within a measurement interval (when $E_s/PT_p = L \geq 1$).

The stationary probability can be numerically computed from the Markov chain, which defines the transition probability matrix $\mathbf{G}(\gamma)$, as follows. $\mathbf{G}(\gamma)$ is a $2(\lceil C/E_s \rceil + 1) \times 2(\lceil C/E_s \rceil + 1)$ matrix that contains $\Pr(B_{n+1}, U_{n+1} | B_n, U_n, \gamma)$ as its elements and is explicitly specified in Appendix A.

The steps involved are: (i) Compute $\mathbf{G}^K(\gamma)$. (ii) Then, compute the probability $\Pr(B_{(m+1)K} | B_{mK}, \gamma)$ that the EHS node has energy $B_{(m+1)K}$ at the end of the m th measurement interval given the SNR, γ , and B_{mK} as $\sum_{u=0}^1 \Pr(B_{(m+1)K}, U_{(m+1)K} = u | B_{mK}, U_{mK} = 0, \gamma)$. (iii) The stationary probabilities are obtained by solving

$$\pi(j) = \sum_i \mathbf{E}_\gamma [\Pr(B_{(m+1)K} = jE_s | B_{mK} = iE_s, \gamma)] \pi(i). \quad (5)$$

The above equation follows from the independence between the energy state at the beginning of a measurement interval and the channel state during the interval.

2) *Fast Fading*: For fast fading, the analysis is simpler because the battery energy state at the beginning of a slot is independent of the channel gain in that slot. Hence, P_{out} and \mathbf{G} are no longer dependent on γ . Therefore, the outage probability now equals $P_{\text{out}}(K) = \sum_i \pi(i) P_{\text{out}}(K|i)$. Here, $P_{\text{out}}(K|i)$ is now given by the recursion:

$$P_{\text{out}}(K|i) = \begin{cases} \sum_{r=0}^K \binom{K}{r} \rho^r (1-\rho)^{K-r} \mathbf{E}_\gamma [P_e(\gamma)]^{\lfloor \frac{i+r}{L} \rfloor}, & i \leq L-1 \\ \rho \mathbf{E}_\gamma [P_e(\gamma)] P_{\text{out}}(K-1|i-L+1) \\ \quad + (1-\rho) \mathbf{E}_\gamma [P_e(\gamma)] P_{\text{out}}(K-1|i-L), & i \geq L \end{cases}.$$

In addition, $P_{\text{out}}(0|i) = 1$. The computation of $\pi(j)$ is similar to that for slow fading, except that \mathbf{G} now directly contains channel-averaged entries.

B. Case 2: Excess Energy Harvested ($E_s/PT_p = L \geq 1$)

Now the energy harvested in a slot is sufficient for L transmissions. Again, the process *within a measurement interval and given the SNR, γ* , is a discrete time Markov process, which is shown in Fig. 3.

1) *Slow Fading*: As before, the state consists of the energy state B_n (normalized with respect to PT_p) and the feedback states U_n . The transition probability matrix $\mathbf{G}(\gamma)$ is given in Appendix B.

The outage probability, as a function of $K \geq 1$, and conditioned on $B_{mK} = iE_s$ and γ , is given by the following recursion relation:

$$P_{\text{out}}(K|i, \gamma) = \begin{cases} \rho P_e(\gamma) P_{\text{out}}(K-1|L-1, \gamma) \\ \quad + (1-\rho) P_{\text{out}}(K-1|0, \gamma), & i = 0 \\ \rho P_e(\gamma) P_{\text{out}}(K-1|i+L-1, \gamma) \\ \quad + (1-\rho) P_e(\gamma) P_{\text{out}}(K-1|i-1, \gamma), & i > 0 \\ P_e^K(\gamma), & i \geq K \end{cases}.$$

In addition, $P_{\text{out}}(K|i, \gamma) = 1$ for $K = 0$. The reasoning behind the above relations is similar to that in Sec. IV-A1.

2) *Fast Fading*: The recursion relations get modified along lines similar to that in Sec. IV-A2, and are not repeated here.

C. Energy Unconstrained Regime

It is instructive to consider when the energy harvested is more than sufficient to handle the communication energy requirements. For example, at high ρ the probability of not having energy to transmit will be low at any time. When this probability becomes zero, *i.e.*, the node in steady state always has sufficient energy to transmit, it is said to be in an *energy unconstrained* regime. In such a case, the outage probability depends only on the transmit energy and is independent of E_s . And, no stationary distribution exists for the Markov chain.

Insights can be obtained by analyzing the $C = \infty$ case. The energy unconstrained regime is characterized as follows:

Proposition 2: An EHS node in a slow fading wireless link operates in the energy unconstrained regime when

$$\rho \geq \frac{1}{K} \frac{PT_p}{E_s} \mathbf{E}_\gamma \left[\frac{1 - (P_e(\gamma))^K}{1 - P_e(\gamma)} \right]. \quad (6)$$

For fast fading, the energy unconstrained regime occurs when

$$\rho \geq \frac{1}{K} \frac{PT_p}{E_s} \frac{1 - (\mathbf{E}_\gamma [P_e(\gamma)])^K}{1 - \mathbf{E}_\gamma [P_e(\gamma)]}. \quad (7)$$

Proof: The proof is given in Appendix C. ■

The above generalizes to continuous valued energy harvest models. Asymptotically, as $E_s \rightarrow \infty$ and E_s/PT_p is kept fixed, the above result simplifies to the intuitively obvious inequality $\rho \geq \frac{PT_p}{KE_s}$. This holds for both slow and fast fading. Note that if $PT_p > KE_s$ then the EHS node cannot operate in the energy unconstrained regime for any value of ρ .

V. SIMULATIONS AND DISCUSSION

We now plot the analytical results and verify them with Monte Carlo simulations that use up to 10^7 samples. The parameters are $T_m = 100$ msec, $D = 32$ bits, $S = 18$ bits [10], $T_s = 0.5$ msec, and $K = 4$. E_s is normalized, without loss of generality, by multiplying it with $(\frac{d_0}{d})^\eta \frac{1}{N_0}$.²

²For example, $E_s = 35$ dB corresponds to an SNR of 18 dB when $P = 1.34$ mW, $T_s = 0.5$ msec, distance $d = 40d_0$, a noise temperature of 300 K, and a bandwidth of 1 MHz.

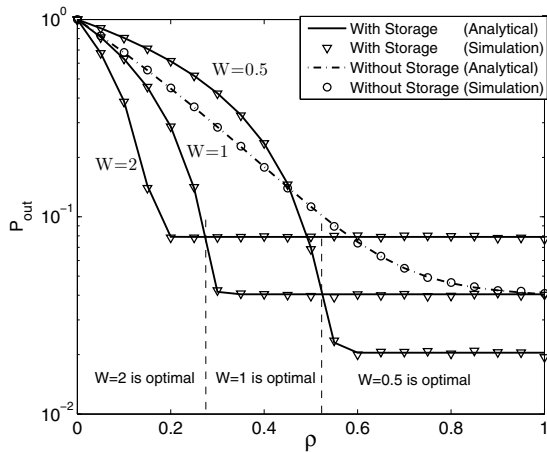


Fig. 4. Outage probability vs. energy injection probability as a function of $W = \frac{E_s}{PT_p}$ for $E_s = 35$ dB, $C = 50E_s$, and slow fading.

Figure 4 plots the outage probability as a function of the energy injection probability, ρ , for $E_s = 35$ dB with and without energy storage. The effect of the parameter $W = E_s/PT_p$ is also shown. The figure brings out several interesting facts. As ρ increases, P_{out} decreases. But, it undergoes a sharp transition to a fixed value when ρ lies in the energy unconstrained regime. This is because P_{out} is now dominated by the packet decoding errors, which depend only on the transmit energy and not ρ .

Different values of W turn out to be optimal for different ρ . For example, $W = 2$ performs best for $0 \leq \rho \leq 0.275$. In other words, for lower injection probabilities, the best strategy is to set the transmit power such that multiple packet transmissions are possible. On the other hand, for $\rho \geq 0.525$, a lower value of W is better since communication reliability and not energy availability is the main obstacle. However, for W lower than $1/K$, the energy unconstrained regime can never be reached. Hence it will have a large outage probability for all values of ρ . Note also that $W = 1$ always performs better than not having storage. This is because storage enables the node to accumulate energy once it has received an ACK.

Figure 5 plots the outage probability as a function of ρ for different battery storage capabilities with $PT_p = E_s$ ($W = 1$). As the battery capacity increases, the outage probability decreases, which is to be expected. However, the gains diminish for larger C . As a bench mark, the no-storage case is also plotted. We again see that even a minimal storage capability reduces the outage probability significantly.

A. Characterization of ρ and System Parameter Optimization

Thus far, in Fig. 4, we varied ρ and E_s separately and studied their individual impact on the EHS link performance. In practice, there exists a relationship between ρ and E_s that depends on the physics of the harvesting mechanism. Since even an empirical characterization is unavailable to the best of our knowledge, we develop an heuristic model that is motivated by the Chernoff bound [12]. Specifically, we use the

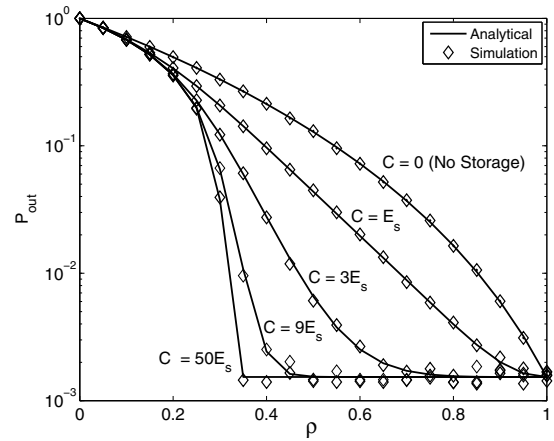


Fig. 5. Outage probability for different values of battery storage capacity, C , for $E_s = 35$ dB, $W = 1$, and fast fading.

relation $\rho = b \exp(-aE_s)$. A larger value of a corresponds to a EHS node that has less energy availability (and, therefore, a lower ρ). While this is correct for large E_s values, we shall assume that this holds even for $E_s \geq 0$ (which forces b to be unity) to gain some insight.

Using this relationship, Fig. 6 plots P_{out} as a function of the transmit energy PT_p for different normalized E_s values. The points with markers correspond to cases where $W = E_s/PT_p$ is an integer, and can, therefore, be analyzed using the results in the previous section. As PT_p increases, the probability of outage first decreases as the communication reliability improves. At the same time, for larger PT_p values, the energy injection probability decreases. Eventually, for larger PT_p , the energy unavailability negatively impacts performance. The key point to note is that PT_p has a significant impact on P_{out} , and must therefore be optimized carefully.

Also, note that for each normalized E_s value, we have a optimal transmission strategy that minimizes outage. In an energy-starved environment with low E_s values (e.g., $E_s = 20$ dB), it is better to operate at $W < 1$ to improve the odds that the packet reaches the destination, even if it is sent less frequently. Similarly, when E_s is high (e.g., $E_s = 32$ dB), $W > 1$ is optimal as this enables more packet transmissions.

VI. CONCLUSIONS

We analyzed the communication performance, in terms of outage probability, for an EHS node that harvests energy sporadically from the environment and uses it to transmit its measurements to a destination over a single-hop time-varying fading channel. Our goal was to minimize the probability that the EHS node fails to deliver its measurements even after possibly multiple retransmissions. We saw that system parameters such as ρ and E_s , which are governed by the energy profile of the node, and its transmission parameters such as P , T_p , and $W = E_s/PT_p$ determine the link performance. Fast fading, if present, improves performance because of the time diversity it provides. Using a heuristic relationship between E_s and ρ , we

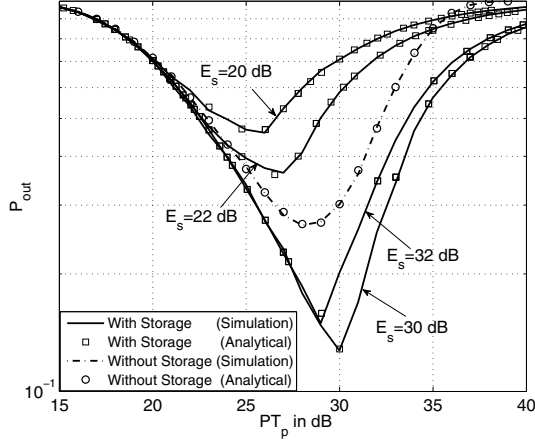


Fig. 6. When ρ and E_s are related: Outage probability vs. transmit energy per packet (PT_p) for different values of normalized E_s for $a = 0.001$, $C = 50E_s$, and slow fading.

also saw that the performance is sensitive to the transmit power settings. Even a minimal amount of energy storage capability was found to reduce outage probability significantly.

The insights were obtained using a simple model amenable to analysis that captured the interactions between the important parameters that govern the EHS link performance. Future work involves refining the model to incorporate multiple levels of harvested energy and time correlations, and evaluating the impact of channel coding on the measurement packets.

APPENDIX

A. Transition Probability Matrix $\mathbf{G}(\gamma)$ for $E_s/PT_p = 1/L$

The element of the state transition matrix $\mathbf{G}(\gamma)$ that corresponds to the transition from (i, r) to (j, s) equals

$$G_{ij}^{rs}(\gamma) = \Pr(B_{n+1} = j, U_{n+1} = s | B_n = i, U_n = r, \gamma),$$

where $i, j \in \{0, 1, \dots, \infty\}$ and $r, s \in \{0, 1\}$. Notice that the transition probabilities depend on the SNR, γ , because the ACK probability does. The equations below are for $C = \infty$. They can be modified suitably for finite C .

For $0 \leq i \leq L-2$ and $r = 0, 1$; or $r = 1$ and $i \geq L-1$: we have $G_{ij}^{rs}(\gamma) = 1 - \rho$, if $j = i$ and $s = 0$; $G_{ij}^{rs}(\gamma) = \rho$, if $j = i + 1$ and $s = 0$; and $G_{ij}^{rs}(\gamma) = 0$ otherwise.

For $i = L-1$ and $r = 0$: we have $G_{ij}^{rs}(\gamma) = 1 - \rho$, if $j = L-1$ and $s = 0$; $G_{ij}^{rs}(\gamma) = \rho(1 - P_e(\gamma))$, if $j = 0$ and $s = 1$; $G_{ij}^{rs}(\gamma) = \rho P_e(\gamma)$, if $j = 0$ and $s = 0$; and $G_{ij}^{rs}(\gamma) = 0$ otherwise.

For $i \geq L$ and $r = 0$: we have $G_{ij}^{rs}(\gamma) = (1 - \rho)P_e(\gamma)$, if $j = (i - L)$ and $s = 0$; $G_{ij}^{rs}(\gamma) = \rho P_e(\gamma)$, if $j = (i - L + 1)$ and $s = 0$; $G_{ij}^{rs}(\gamma) = (1 - \rho)(1 - P_e(\gamma))$, if $j = (i - L)$ and $s = 1$; $G_{ij}^{rs}(\gamma) = \rho(1 - P_e(\gamma))$, if $j = (i - L + 1)$, $s = 1$; and $G_{ij}^{rs}(\gamma) = 0$ otherwise.

B. Transition Probability Matrix $\mathbf{G}(\gamma)$ for $E_s/PT_p = L$

For $i \geq 1$ and $r = 0$: we have $G_{ij}^{rs}(\gamma) = \rho P_e(\gamma)$, if $j = i + L - 1$ and $s = 0$; $G_{ij}^{rs}(\gamma) = \rho(1 - P_e(\gamma))$, if $j = i + L - 1$

and $s = 1$; $G_{ij}^{rs}(\gamma) = (1 - \rho)P_e(\gamma)$, if $j = i - 1$ and $s = 0$; $G_{ij}^{rs}(\gamma) = (1 - \rho)(1 - P_e(\gamma))$, if $j = i - 1$ and $s = 1$; and $G_{ij}^{rs}(\gamma) = 0$ otherwise.

For $i = 0$ and $r = 0$: we have $G_{ij}^{rs}(\gamma) = 1 - \rho$, if $j = 0$ and $s = 0$; $G_{ij}^{rs}(\gamma) = \rho P_e(\gamma)$, if $j = L - 1$ and $s = 0$; $G_{ij}^{rs}(\gamma) = \rho(1 - P_e(\gamma))$, if $j = L - 1$ and $s = 1$; and is 0 otherwise.

For $i \geq 0$ and $r = 1$: we have $G_{ij}^{rs}(\gamma) = 1 - \rho$, if $j = i$ and $s = 1$; $G_{ij}^{rs}(\gamma) = \rho$, if $j = i + L$ and $s = 1$; and $G_{ij}^{rs}(\gamma) = 0$ otherwise.

C. Proof of Proposition 2

We first analyze slow fading. In the energy unconstrained regime, it is easy to see that exactly i transmissions occur in a measurement interval with SNR, γ , with probability $(1 - P_e(\gamma))(P_e(\gamma))^{i-1}$. Therefore, the average energy consumed in an interval equals PTK_{av} , where $K_{av} = \mathbf{E}_\gamma \left[(1 - P_e(\gamma)) \sum_{i=1}^{K-1} i (P_e(\gamma))^{i-1} + K (P_e(\gamma))^{K-1} \right]$. Comparing this with the average energy injected in a measurement interval, $\rho E_s \left(\frac{T_m}{T_p} \right)$, yields the desired expression. For fast fading, the reasoning is similar except that $P_e(\gamma)$ is replaced by its channel-averaged equivalent.

REFERENCES

- [1] J. A. Paradiso and T. Starner, "Energy scavenging for mobile and wireless electronics," *IEEE Trans. Pervasive Comput.*, pp. 18–27, Jan.–Mar. 2005.
- [2] D. Niyato, E. Hossain, and A. Fallahi, "Sleep and wakeup strategies in solar-powered wireless sensor/mesh networks: Performance analysis and optimization," *IEEE Trans. Mobile Comput.*, vol. 6, pp. 221–236, Feb. 2007.
- [3] M. Tacca, P. Monti, and A. Fumagalli, "Cooperative and reliable ARQ protocols for energy harvesting wireless sensor nodes," *IEEE Trans. Wireless Commun.*, vol. 6, pp. 2519–2529, July. 2007.
- [4] C. R. Murthy, "Power Management and Data Rate Maximization in Wireless Energy Harvesting Sensors," *Int. J. Wireless Information Networks*, vol. 16, pp. 102–117, Jul. 2009.
- [5] J. Lei, R. Yates, and L. Greenstein, "A generic model for optimizing single-hop transmission policy of replenishable sensors," *IEEE Trans. Wireless Commun.*, vol. 8, pp. 547–551, Feb. 2009.
- [6] A. Kansal, J. Hsu, S. Zahedi, and M. B. Srivastava, "Power management in energy harvesting sensor networks," *ACM Trans. Embedded Comput. Syst.*, vol. 7, pp. 1–38, Sept. 2007.
- [7] J. Ammer and J. Rabaey, "Low power synchronization for wireless sensor network modems," in *Proc. WCNC*, pp. 670–675, 2005.
- [8] B. Medepally, "Link design for energy harvesting sensors," Master's Thesis, Indian Institute of Science, 2009.
- [9] S. Cui and A. J. Goldsmith, "Cross-layer design in energy-constrained networks using cooperative MIMO techniques," *EURASIP Signal Processing Journal, Special Issue on Advances in Signal Processing-based Cross-layer Designs*, vol. 86, pp. 1804–1814, Aug. 2006.
- [10] J. A. Paradiso and M. Feldmeier, "A compact, wireless, self powered pushbutton controller," in *Proc. Int. Conf. Ubiquitous Comput.*, pp. 299–304, 2001.
- [11] I. S. Gradshteyn and I. M. Ryzhik, *Table of Integrals, Series and Products*. Academic Press, 4th ed., 1980.
- [12] J. G. Proakis, *Digital Communications*. McGraw-Hill, 2nd ed., 1989.
- [13] R. M. Radaydeh and M. M. Matalgah, "Results for infinite integrals involving higher-order powers of Q-function with application to average SEP analysis of DE-QPSK," *IEEE Trans. Wireless Commun.*, pp. 670–675, Mar. 2008.